Geofísica Internacional (1995), Vol. 34, Num. 1, pp. 131-141

Hypocentral cross-sections and arc-trench curvature

Marco Guzmán-Speziale
Instituto de Geofísica, UNAM
México

Received: June 10, 1994; accepted: September 26, 1994.

RESUMEN

Se presenta un método para obtener el centro de curvatura (polo) así como los puntos de inflexión de trincheras sobre una Tierra esférica. Dicha información es necesaria para proyectar secciones hipocentrales sobre el arco (trinchera) o perpendicular a él. Este tipo de proyecciones permite una caracterización más exacta de la zona de Wadati-Benioff que el método tradicional de la linea recta. También se presentan las expresiones de proyección arqueada para tenerlas como referencia. Se calculan, como ejemplo, los polos y puntos de inflexión de la trinchera mesoamericana. Esta información es usada para obtener secciones hipocentrales de esta zona a fin de compararlas con secciones tradicionales ya publicadas.

PALABRAS CLAVE: Perfiles hipocentrales, curvatura de la trinchera.

ABSTRACT

A method is shown for obtaining the center of curvature, or pole, as well as the points of inflection of arcuate features such as trenches, on a spherical Earth. This information is needed, among other things, for projecting hypocenters along the arc or perpendicular to it, which is better for depicting the geometry of Wadati-Benioff zones than the traditional straight-line approach. As a reference, the basic expressions for arcuate hypocentral projections are also given. As an example, the poles and points of inflection for the Middle America Trench are obtained. Using these parameters, hypocentral cross-sections projected along the arc and perpendicular to it for this region are shown. The advantage of such sections as compared to straight-line sections from the literature is demonstrated.

KEY WORDS: Hypocentral cross-sections, trench curvature.

INTRODUCTION

Traditionally, hypocentral cross-sections have been obtained by projecting hypocenters perpendicularly onto a plane normal to the surface of the Earth. Examples of this kind of projection abound in the literature, from classic papers [e.g., Benioff, 1954; Isacks *et al.*, 1968; Isacks and Barazangi, 1977] to more recent ones [e.g, Taylor and Karner, 1983; Burbach *et al.*, 1984; Burbach and Frohlich, 1986; Cahill and Isacks, 1992; Ponce *et al.*, 1992; Suárez and Comte, 1993; Kao and Chen, 1994]. Projecting hypocenters along or across an arcuate feature [e.g., Kawakatsu, 1986; Ekström and Engdahl, 1989; Engdahl *et al.*, 1989] is a reasonable approach if one wishes to study features related to the curvature of the Earth or to the curvature of trenches, such as the geometry of a subducted slab or the position of a volcanic arc relative to a trench.

Hypocentral projection along (or across) an arcuate features is an exercise in elementary geometry if the curvature of the feature (or equivalently the center of curvature) is known. It is the purpose of this note to: (1) Present a method to obtain the location of the centers of curvature (or poles) for segments of constant curvature along a trench; (2) Show how to locate the points of inflection between such segments; (3) Provide basic unpublished expressions for projecting hypocenters (either along the arc or perpendicular to it); 4) Show examples for the Middle America Trench in which we compare published straight-line projections with arcuate projections.

METHOD

Turcotte and Schubert [1982] and Yamaoka and Fukao [1987] suggest that ocean trenches may be divided into segments of constant curvature, which represent arcs of small circles on a sphere. For simplicity, we call these segments *arcs*.

We begin by digitizing the trench of interest. Next we visually inspect it and divide it into tentative segments of constant curvature. For each arc a center of curvature, or *pole*, is obtained, using only points that definitely fall on a single arc. Areas near a change of curvature (inflection points) must be avoided because at this stage the location of each inflection point is not known.

Inflection points between arcs are located next. Each arc is now completely defined by its center of curvature and its two inflection points with neighboring arcs (Figure 1a). In general, this procedure yields statistically good results at the first try.

In what follows we discuss how to obtain the center of curvature and the points of inflection for each arc. We also provide expressions for projection along or perpendicular to arcuate features.

Center of curvature and points of inflection

Let $\mathbf{x}=(x_1,x_2,x_3)$ be the Cartesian coordinates of the pole to be determined. Let $\mathbf{y}=(y_1,y_2,y_3)$ and $\mathbf{z}=(z_1,z_2,z_3)$ be

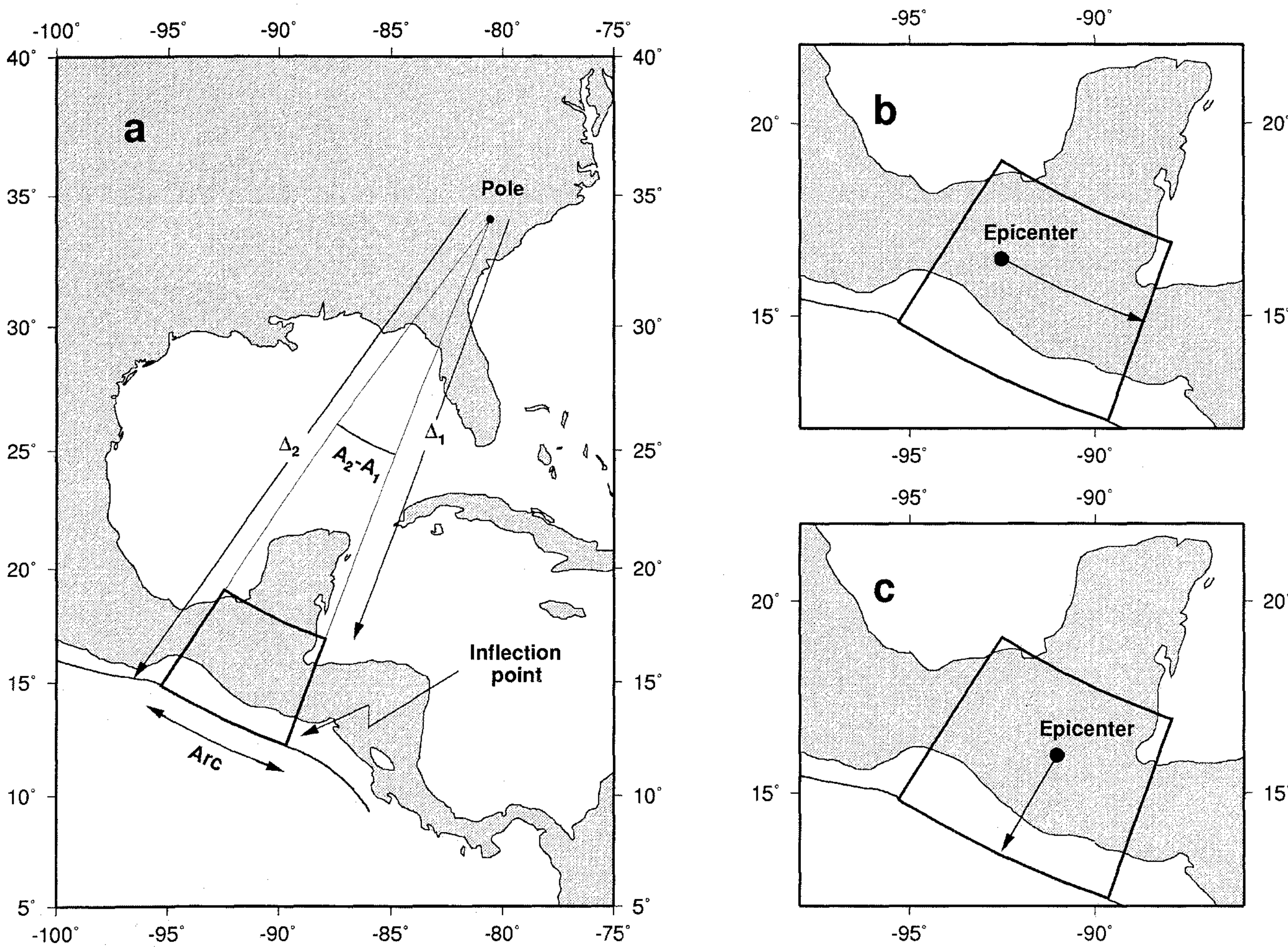

Fig. 1. a) Parameters related to arc-trench curvature and used for projecting hypocenters along the arc or perpendicular to it. An additional parameter not shown is the depth of the earthquake. b) Projection perpendicular to the arc is performed through a small circle centered at the pole. c) Hypocenters are projected along the arc through a great circle which passes trough the pole and the epicenter. The arc itself is later *unrolled* to obtain a two-dimensional view. See text for details. Figures (except those from Burbach *et al.*, 1984) were generated using the GMT mapping programs [Wessel and Smith, 1991].

the coordinates of any two points along the arc. All three points are located on the surface of the Earth and **y** and **z** are known. For convenience, we consider the Earth to be a sphere of radius unity. Thus all position vectors **x**, **y**, and **z** are unit vectors.

The angular distance at the center of the Earth from the pole to any point on the arc is constant and equal to the dot product between the corresponding position vectors. Thus:

$$\mathbf{x}\cdot\mathbf{y}=\mathbf{x}\cdot\mathbf{z} \tag{1}$$

From (1) we may define the total least-square error for all points along the arc as

$$e^2=\sum_{i=1}^{N}[(\mathbf{x}\cdot\mathbf{y})-(\mathbf{x}\cdot\mathbf{z})]^2\ , \tag{2}$$

where N is half the number of digitized points because we are taking pairs of points along the arc (**y** and **z**) at the same time. In practice, we take the first half to be the **y**'s and the last half the **z**'s. We minimize (2) to solve for **x**, which leads to the homogeneous system of equations

$$\mathbf{A}\ \mathbf{x}=\mathbf{0} \tag{3a}$$

where the symmetric matrix of coefficients is

$$\mathbf{A}=\begin{bmatrix}\sum(y_1-z_1)^2 & \sum(y_1-z_1)(y_2-z_2) & \sum(y_1-z_1)(y_3-z_3)\\ \sum(y_1-z_1)(y_2-z_2) & \sum(y_2-z_2)^2 & \sum(y_2-z_2)(y_3-z_3)\\ \sum(y_1-z_1)(y_3-z_3) & \sum(y_2-z_2)(y_3-z_3) & \sum(y_3-z_3)^2\end{bmatrix} \tag{3b}$$

with all summations from *1* to *N*.

Instead of trying to solve for **x** directly from (3), we may take advantage of some properties of homogeneous systems of equations and symmetric matrices.

For a homogeneous system of equations to have a non-trivial solution its matrix of coefficients must be singular. A matrix is singular if, and only if, at least one of its eigenvalues (λ) is zero [e.g., Wylie and Barrett, 1982, p. 718]. Thus, for the system defined by (3) to have a non-trivial solution at least one of the eigenvalues of **A** must be zero. At the same time, the eigenvector of **A** corresponding to λ=0 is directly a solution of (3) because the characteristic equation

$$[\mathbf{A}-\lambda\mathbf{I}][\mathbf{x}]=[\mathbf{0}] \tag{4}$$

becomes identical with (3) when we substitute for λ=0.

A simple way to find eigenvalues and eigenvectors of a symmetric matrix is by using Jacobi (orthogonal similarity) transformations. For a 3×3 matrix these are rotations about one of the coordinate axis [e.g., Press *et al.*, 1986]. This method allows the three eigenvalues and their corresponding eigenvectors to be found at the same time. The eigenvector corresponding to λ=0 will be the center of curvature.

The location of a pole thus obtained is considered satisfactory if the average deviation defined as

$$Adev=\frac{1}{N}\sum_{i=1}^{N}\left|\Delta_i-\overline{\Delta}\right| , \tag{5}$$

[Press *et al.*, 1986] is less than 0.1°. Here Δ_i is the angular distance from the ith point of the arc to the pole and $\overline{\Delta}$ is the average distance. Where curvature is large, such as in the Marianas, the distance from the center of curvature to the arc is in the order of 5°; thus an average deviation of 0.1° represents an error of 2 %. For more typical pole-arc distances of the order of 10° (such as in the Middle America Trench; Table 1), this average deviation means that relative errors are around 1 %.

Once the centers of curvature are determined, the points of inflection are found in a simple manner. The point where two arcs intersect (i.e., the point of inflection) belongs to both arcs, whether they meet tangentially (as in the Middle America Trench) or whether they cross, forming a cusp (as in Kamchatka, for example). We take advantage of this fact to locate the inflection points.

Consider two neighboring arcs, a_1 and a_2, and their respective poles P_1 and P_2. Let δ_1 be the angular distance from P_1 to a_1, and δ_2 the distance from P_2 to a_2. If the inflection point belongs to both arcs its distance to P_1 will be δ_1 and at the same time its distance to P_2 will be δ_2. The location of the inflection point is found by the inverse procedure, i.e., searching for a point along the trench such that the distance to P_1 is δ_1 and the distance to P_2 is δ_2.

Projection of hypocenters

In this section we show the basic expressions for projecting hypocenters perpendicular to the arc or along it. For sections perpendicular to the arc the hypocenters are projected through small circles with center at the pole onto a plane perpendicular to the arc. That is, hypocenters are projected as a function of their latitude with respect to the pole and of depth, holding constant their longitude with respect to the pole (Figure 1b).

Projection along the arc is a two-step process. First, the hypocenters are projected onto the arc as a function of their longitude and depth with respect to the pole, that is, through great circles from the pole to the arc (Figure 1c). But the arc itself is a curved surface; thus the next step is projecting this curved surface onto a plane.

A hypocenter is selected for projection if it falls within certain prescribed limits in regard to latitude (angular distance subtended at the center of the Earth) and longitude (azimuth) with respect to the pole. A third dimension may be added by restricting the depth of the earthquakes to be projected. Let Δ_1 and Δ_2 be the minimum and maximum angular distances from the pole. Let A_1 and A_2 be the minimum and maximum azimuth from the pole (Figure 1a) and H the maximum depth. For each individual earthquake, δ is the angular distance from the pole, α the azimuth from the pole, and z the depth.

Projection on paper is achieved by plotting each hypocenter as a function of the proper spherical parameters,

Table 1

Parameters for arc-like segments along the Middle America Trench

N	Pole		Δ (°)	Adev (°)	Initial point		Final point	
	Lat	Lon			Lat	Lon	Lat	Lon
1	20.89	-103.70	2.77	0.007	21.16	-106.70	18.62	-105.38
2	33.13	-93.21	18.19	0.060	18.62	-105.38	15.11	-96.09
3	13.15	-96.32	2.00	0.005	15.11	-96.09	14.84	-95.24
4	34.10	-80.55	23.41	0.016	14.84	-95.24	12.19	-89.64
5	5.37	-92.00	7.18	0.016	12.19	-89.64	9.31	-85.95

depending on what kind of projection is desired (along the arc or perpendicular to it). As most plotting packages for computers work with Cartesian coordinates it is convenient to convert hypocentral coordinates to these coordinates. For projection perpendicular to the arc, the Cartesian coordinates of a projected hypocenter are

$$x = x_1 - [(R - z) \cdot \sin\theta] \tag{6a}$$

$$y = y_1 + [(R - z) \cdot \cos\theta] \tag{6b}$$

where R is the radius of the Earth, and

$$\theta = \frac{\Delta_1 + \Delta_2}{2} - \delta \tag{7a}$$

$$x_1 = R \cdot \sin[(\Delta_2 - \Delta_1)/2] \tag{7b}$$

$$y_1 = (H - R) \cdot \cos[(\Delta_2 - \Delta_1)/2] \tag{7c}$$

The Cartesian coordinates of projection along the arc are

$$x = x_2 - [(R - z) \cdot \cos(\gamma + \beta)] \tag{8a}$$

$$y = y_2 + [(R - z) \cdot \sin(\gamma + \beta)] \tag{8b}$$

where

$$x_2 = R \cdot \sin[(A_2 - A_1) \cdot \sin\Delta_2 / 2] \tag{9a}$$

$$y_2 = (H - R) \cdot \cos[(A_2 - A_1) \cdot \sin\Delta_2 / 2] \tag{9b}$$

$$\beta = (\alpha - A_1) \cdot \sin\Delta_2 \tag{9c}$$

$$\gamma = \cos^{-1}(x_2 / R) \tag{9d}$$

Coordinates for projection along the arc already take into account the projection of the curved arc onto a plane.

AN EXAMPLE: THE MIDDLE AMERICA TRENCH

The geometry of the Cocos Plate, as it is being subducted along the Middle America Trench (MAT), has been studied in some detail [e.g., Hanus and Vanek, 1978; Burbach *et al.*, 1984; Pardo, 1993]. The dip of subduction changes along the MAT, from around 20° in the northwestern portion, deepening to some 40°-50° along Central America [e. g., Bevis and Isacks, 1984]. The change in curvature at different places along the MAT prevents a good depiction of the geometry of the subducted Cocos Plate when straight-line cross-sections are used, such as in the studies mentioned above. We use this region as an example of how the center of curvature and inflection points may be calculated and what advantages may be obtained when arcuate projection is used along areas of changing curvature.

From visual inspection, we identify five arcs along the MAT. From northwest to southeast, the first one spans the northwestern end of the MAT to about the place where the Rivera Fracture Zone intersects the trench (around 105° W; Figure 2). It is concave towards the continent (negative curvature), with a strong curvature. The second segment is also concave towards the continent, but with a larger radius of curvature. In a bathymetric map (Figure 2) it appears to span from the Rivera Fracture Zone to about 96° W, where the isobath curves broaden and the 3,500 m isobath changes its trend from NW-SE to NE-SW. The next arc includes the Gulf of Tehuantepec (approximately 96° W to 95° W), with a positive (concave seaward) curvature. It ends at the Tehuantepec Fracture Zone (TFZ). The fourth segment is concave landward, and goes from the TFZ to about 88.5° W. It approximately spans the region where the MAT reaches its maximum depth at about 5,500 m. The last segment is concave seaward and spans from about 88.5° W to the southeastern end of the MAT, where it intersects the Cocos Ridge.

We use the method described above to find the centers of curvature (poles) and the points of inflection for the five tentative segments. Results are shown on Figure 2 and Table 1. All segments have an average deviation of less than 0.1°. Actually the largest deviation is 0.06° and the smallest one 0.005°, well within our tolerance. Given the small deviations, we consider that the five segments initially proposed from visual inspection agree well with the arc-like segments. Note that the technique was applied only once, that is, the first visual inspection already yielded all five segments. Interestingly, the inflection point between each segment is marked by a bathymetric feature.

The study of Burbach *et al.* [1984] may serve as a point of departure for comparing straight cross-sections versus arcuate ones. The location of cross-sections along the MAT obtained by these authors is reproduced in Figure 3a. Figure 3b shows an alternative distribution of arcuate-projection cross-sections which span approximately the same area, except for the region around the Isthmus of Tehuantepec (section g'). The same data base is used in both cases: well-located hypocenters reported by the International Seismological Centre (ISC) and compiled by Burbach *et al.* [1984). The correponding cross-sections are shown in Figure 4.

On map view, notice that the arcuate sections provide an improved fit to regions of changing curvature, such as the Isthmus of Tehuantepec. In the straight-line projection (Figure 3a) one must choose between projecting perpendicular to the trench as it trends northwest of the isthmus or southeast of it. Burbach *et al.* [1984] chose the latter. Arcuate projection (Figure 3b), on the other hand, fits the change of curvature of the trench in the area. The difference is important for reasons discussed below.

The position of the trench in cross-section view is more easily determined from arcuate projection: it is always located in the upper-left corner of the section, unless

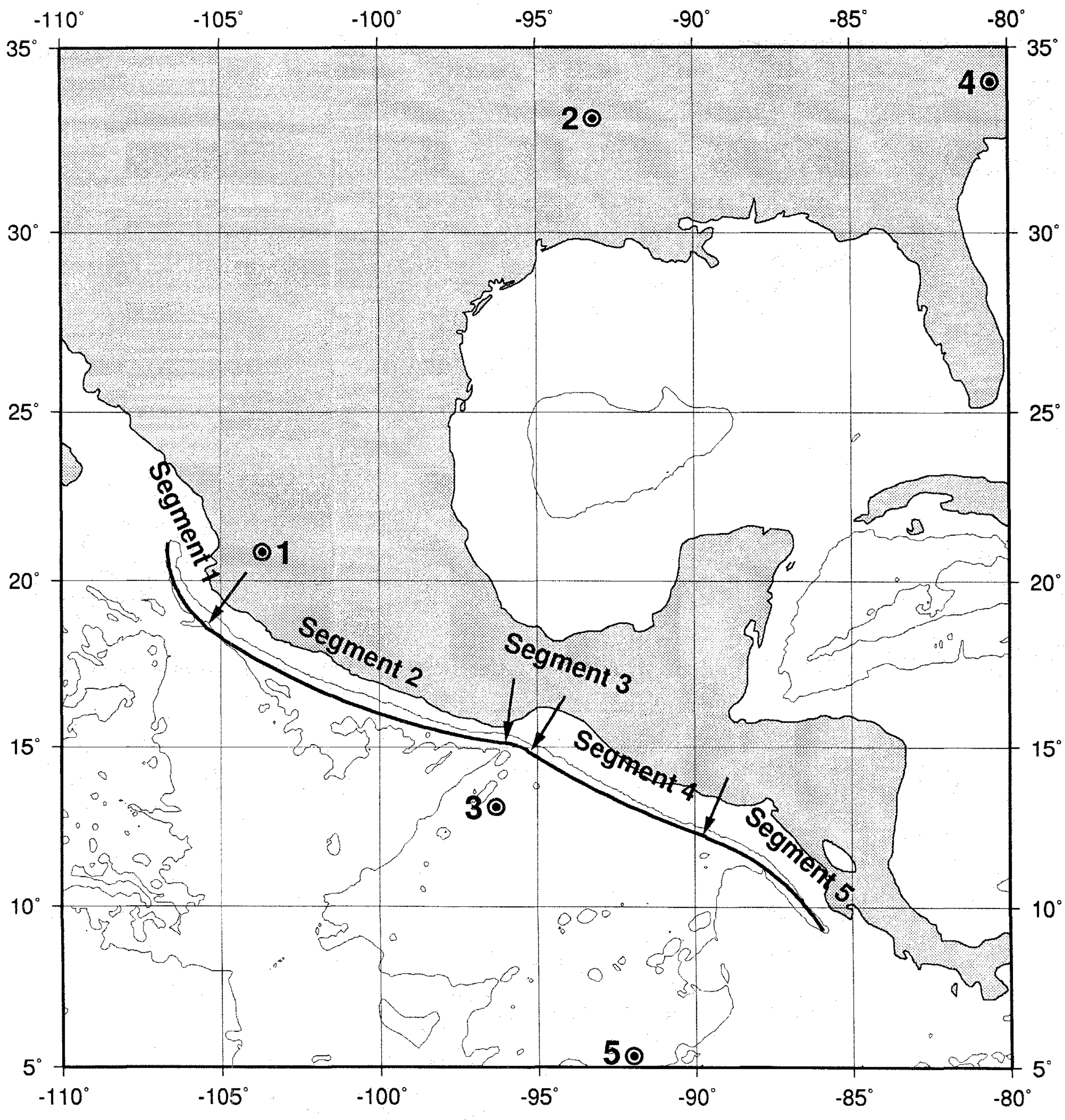

Fig. 2. Segments of constant curvature adjusted to the Middle America Trench. Arrows show location of inflection points and therefore indicate the limit between two neighboring segments. Numbered circles are the centers of curvature for each segment. Light line indicates the 3,500 km depth contour.

one choses to project with respect to a different feature. Furthermore, the position of the trench in a straight-line projection corresponds to the place where the central line of the section crosses the trench. This position is not the same as one moves away from this line. For the arcuate projection, the position of the trench stays the same for the entire projection area (Figures 3 and 4).

There is a well-documented major change in the dip of subduction of the Cocos Plate around the Isthmus of Tehuantepec at about longitude 96° W [Hanus and Vanek, 1978; Bevis and Isacks, 1984]. Northwest of this point, the Cocos plate subducts with a shallow angle of about 20° and reaches far inland, as evidenced by the presence of the Trans-Mexican Volcanic Belt, some 400 km from the MAT. To the southeast, on the contrary, the angle of subduction is steeper (some 45°) and the volcanic chain is close to the trench.

An arcuate projection depicts well this situation (Figures 3 and 4): the change is evident from section g' to section h, right at the Isthmus of Tehuantepec where it takes

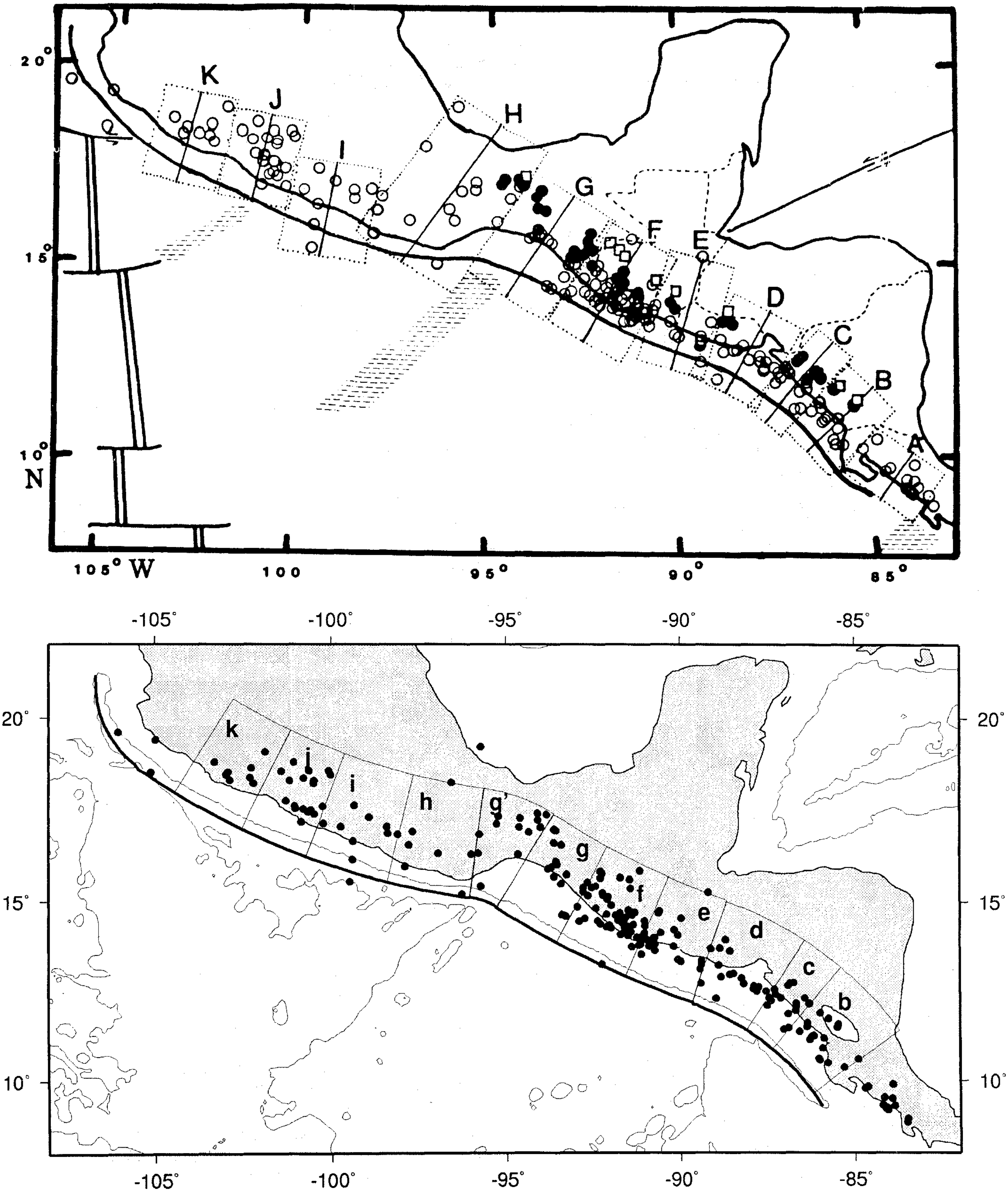

Fig. 3. Location of cross-sections along the Middle America Trench. A) With traditional methodology (from Burbach *et al.*, 1984). B) Using projection perpendicular to the arc. Notice that it is easier to sample the Wadati-Benioff zone around the Isthmus of Tehuantepec (-95° longitude) with arcuate sections.

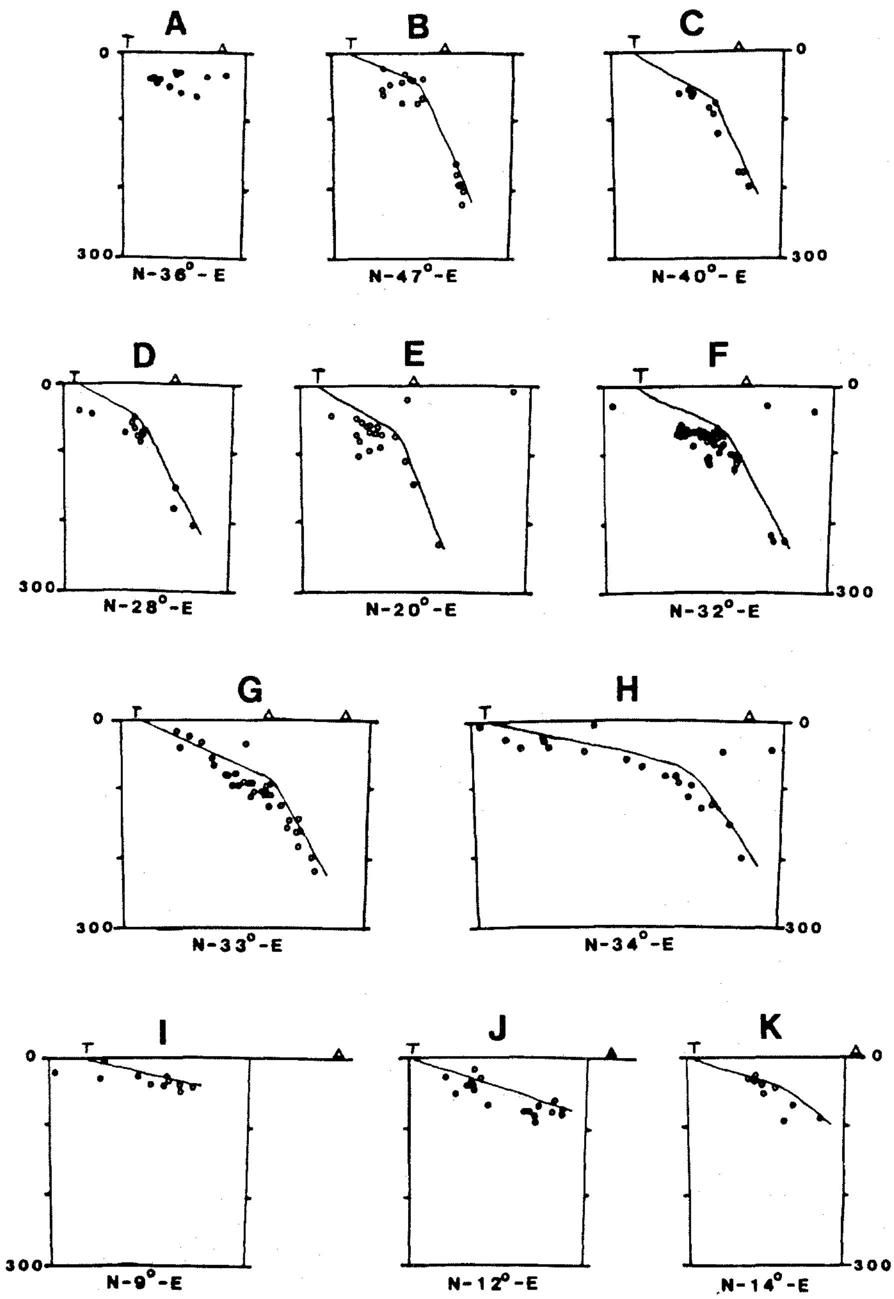

Fig. 4. Cross-sections corresponding to Figure 2. Capital letters indicate traditional sections from Burbach *et al.* [1984]. Sections obtained by arcuate projection are shown with lower-case letters with horizontal tic marks every 100 km and vertical tic marks at 50 km intervals. Refer to Figure 3 for location of sections. Hypocentral data base is the same for both cases. Notice that with arcuate projection there is no need to mark the position of the trench because it is always located in the upper-left corner of the section.

place (see Bevis and Isacks, 1984). Using a straight-line projection, however, this change of dip seems to take place further to the northwest, from section *H* to *I*.

Projection along the arc also shows the advantage of the arcuate as compared with the straight-line methods. In the arcuate projection the entire length of the arc is used whereas in the linear projection one has to select a straight line that best fits the trench. This leads to differences in the length of the section, the arcuate section is always longer. In the case of the MAT, the difference in distance between end points of the section is only 28 km (Figure 5) because of the small curvature of the arc. Much of the MAT has a radius of curvature 20° subtended at the center of the Earth. For arcs with larger curvatures the difference may become critical. In extreme cases, such as the Marianas, the radius

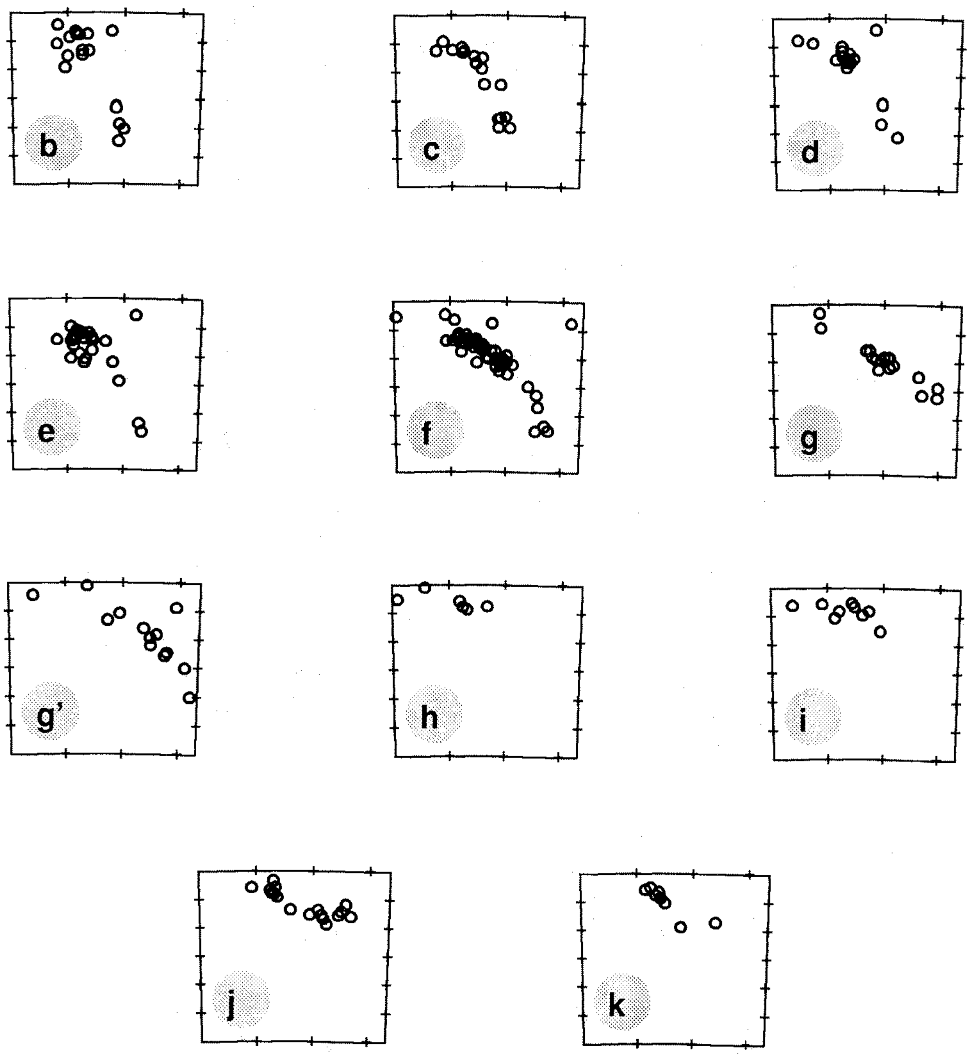

Fig. 4. (Cont.)

of curvature is about 5° with an azimuthal span of more than 180°, thus making it virtually impossible to project the entire arc with a single straight-line projection.

DISCUSSION AND CONCLUSIONS

Depicting a three-dimensional geometry on a plane will always lead to some distortion, no matter which projection is used. In this work we develop a simple method for projecting hypocenters that minimizes distortion when the geometry of the Wadati-Benioff Zone or other trench-related features are studied. This method has several advantages over traditional straight-line methods: (1) It is easier to obtain cross-sections in regions where the curvature of the trench changes abruptly, such as in the Isthmus of Tehuantepec, or in regions of large curvature; (2) The position of the trench is constant for all the section considered; (3) The relative position of a hypocenter with respect to the trench is also constant. There are obviously some instances where straight-line projection may be preferable, such as the study of seismicity associated to strike-slip faults which may be considered straight lines.

The use of the method may be extended to other situations. For example, one may take the Euler vector of a plate pair and take it as the center of curvature in order to study seismicity or plate geometry as a function of age of subduction, or as a function of distance from the Euler pole. In this case the arc would not be the trench (or a portion of it) but the path of convergence.

Other applications are beyond the scope of this paper. As an example, there is a bathymetric feature at each inflection point along the MAT. Is this unique to the MAT or is it found at other trenches? Is there a cause-effect relationship between the location of an inflection point and the

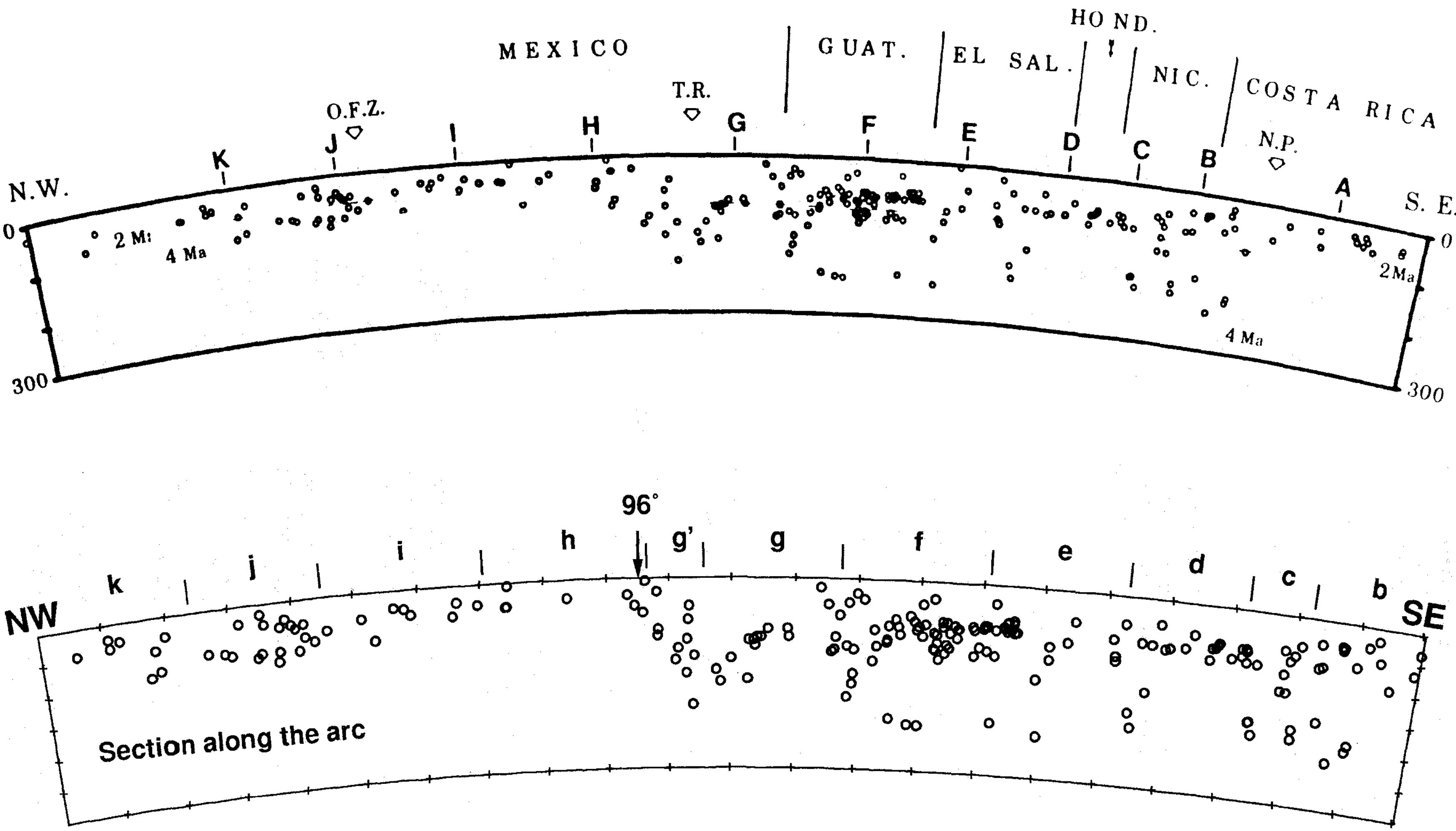

Fig. 5. Sections along the Middle America Arc. Top: straight-line projection. Bottom: arcuate projection along the arc. Notice that, given the relatively small curvature of the MAT there is no appreciable difference between sections.

presence of a bathymetric feature? Other possible topics are: the relationship between trench curvature and subduction geometry before and after subduction, that is, determination of Gaussian curvature [e.g., Bevis, 1986; Cahill and Isacks, 1992]; the state of stress in the subducted slab where the trench curvature changes from concave to convex, etc. The method may also be used to determine the direction normal to the trench, a parameter widely used in studies of oblique convergence [e.g., Burbach and Frohlich, 1986; Jarrard, 1986; McCafrey, 1992].

The method of projection is intuitively very simple and the mathematical expressions are straight-forward. Often there is a clear advantage in using arcuate projection over straight-line projection, as shown by the example of the Middle America Trench.

ACKNOWLEDGEMENTS

Many people made useful suggestions about this manuscript and the method of projection in general. I am grateful to the users of the computer facilities at the Instituto de Geofísica, UNAM, who have made valuable comments leading to important improvements. Thanks also go to two anonymous referees who thoroughly reviewed the manuscript.

BIBLIOGRAPHY

BENIOFF, H., 1954. Orogenesis and deep crustal structure: Additional evidence from Seismology. *Geol. Soc. Am. Bull., 65,* 385-400.

BEVIS, M., 1986. The curvature of Wadati-Benioff zones and the torsional rigidity of subducting plates. *Nature, 323,* 52-53.

BEVIS, M. and B. L. ISACKS, 1984. Hypocentral trend surface analysis: Probing the geometry of Benioff zones. *J. Geophys. Res., 89,* 6153-6170.

BURBACH, G.V.,C. FROHLICH, W.D. PENNINGTON and T. MATUMOTO, 1984. Seismicity and tectonics of the subducted Cocos Plate. *J. Geophys. Res., 89,* 7719-7735.

BURBACH, G.V. and C. FROHLICH, 1986. Intermediate and deep seismicity and lateral structure of subducted lithosphere in the circum-Pacific region. *Rev. of Geophys., 24,* 833-874.

CAHILL, T. and B. L. ISACKS, 1992. Seismicity and shape of the subducted Nazca Plate. *J. Geophys. Res., 97,* 17503-17529.

EKSTRÖM, G. and E. R. ENGDAHL, 1989. Earthquake source parameters and stress distribution in the Adak Island region of the Central Aleutian Islands, Alaska. *J. Geophys. Res., 94,* 15499-15519.

ENGDAHL, E. R., S. BILLINGTON and C. KISSLINGER, 1989. Teleseismically recorded seismicity before and after the May 7, 1986, Andreanof islands, Alaska, earthquake. *J. Geophys. Res., 94,* 15481-15498.

HANUS, V. and J. VANEK, 1978. Subduction of the Cocos Plate and deep active fracture zones of Mexico, *Geofís. Int., 17,* 14-53.

ISACKS, B.L., J. OLIVER and L.R. SIKES, 1968. Seismology and the new global tectonics. *J. Geophys. Res., 73,* 5855-5899.

ISACKS, B. L. and M. BARAZANGI, 1977. Geometry of Benioff zones: Lateral segmentation and downward bending of the subducted lithosphere. *In:* M. Talwani and W. C. Pitman III (Editors), Island arcs, deep sea trenches, and back-arc basins. American Geophysical Union, Washington, 470 pp.

JARRARD, R. D., 1986. Relations among subduction parameters. *Rev. Geophys, 24,* 217-284.

KAO, H. and W-P. CHEN, 1994. The double seismic zone in Kuril-Kamchatka: The tale of two overlapping single zones. *J. Geophys. Res., 99,* 6913-6930.

KAWAKATSU, H., 1986. Downdip tensional earthquakes beneath the Tonga Arc: A double seismic zone? *J. Geophys. Res., 91,* 6432-6440.

McCAFREY, R., 1992. Oblique plate convergence, slip vectors, and forearc deformation. *J. Geophys. Res., 97,* 8905-8915.

PARDO, M., 1993. Características sismotectónicas de la subducción de las placas de Rivera y Cocos en el sur de México. Ph. D. dissertation. Universidad Nacional Autónoma de México, México, DF.

PONCE, L., R. GAULON, G. SUAREZ and E. LOMAS, 1992. Geometry and state of stress of the downgoing Cocos Plate in the Istmus of Tehuantepec, Mexico. *Geophys. Res. Let., 19,* 773-776.

PRESS, W. H., B. P. FLANNERY, S. A. TEUKOLSKY and W. T. VETTERLING, 1986. Numerical Recipes. Cambridge University Press, Cambridge, U.K., 818 pp.

SUAREZ, G. and D. COMTE, 1993. Comment on "Seismic coupling along the Chilean subduction zone" by B. W. Tichelaar and L. R. Ruff. *J. Geophys. Res., 98,* 15825-15828.

TAYLOR, B. and G. D. KARNER, 1983. On the evolution of marginal basins. *Rev. of Geophys. Spac. Phys., 21,* 1727-1741.

TURCOTTE, D.L. and G. SCHUBERT, 1982. Geodynamics applications of continuum physics to geological problems. John Wiley and Sons, New York, 450 pp.

YAMAOKA, K. and Y. FUKAO, 1987. Why do island arcs form cusps at their junction? *Geology, 15*, 34-36.

WESSE, P. and W. H. F. SMITH, 1991. Free software helps map and display data. *EOS Trans. AGU, 72*, 441, 445-446.

WYLIE, C. R. and L. C. BARRET, 1982. Advanced Engineering Mathematics. McGraw-Hill Book Company, New York, 1103 pp.

Marco Guzmán-Speziale
Instituto de Geofísica, UNAM, Cd. Universitaria, 04510 México DF, México.